A Capillary Gel Electrophoresis–Coupled Aptamer Enzymatic Cleavage Protection Strategy for the Simultaneous Detection of Multiple Small Analytes.

ARTICLE *in* ANALYTICAL CHEMISTRY · APRIL 2014

Impact Factor: 5.64 · DOI: 10.1021/ac5010234 · Source: PubMed

6 AUTHORS, INCLUDING:

Perrier Sandrine
University Joseph Fourier - Grenoble 1
19 PUBLICATIONS **383** CITATIONS
SEE PROFILE

Corinne Ravelet
University Joseph Fourier - Grenoble 1
48 PUBLICATIONS **898** CITATIONS
SEE PROFILE

Valérie Guieu
University Joseph Fourier - Grenoble 1
22 PUBLICATIONS **434** CITATIONS
SEE PROFILE

Eric Peyrin
University Joseph Fourier - Grenoble 1
107 PUBLICATIONS **1,825** CITATIONS
SEE PROFILE

analytical chemistry

Article

pubs.acs.org/ac

Capillary Gel Electrophoresis-Coupled Aptamer Enzymatic Cleavage Protection Strategy for the Simultaneous Detection of Multiple Small Analytes

Sandrine Perrier, Zhenyu Zhu, Emmanuelle Fiore, Corinne Ravelet, Valérie Guieu, and Eric Peyrin*

Université Grenoble Alpes, DPM UMR 5063, F-38041 Grenoble, France

CNRS, DPM UMR 5063, F-38041 Grenoble, France

Supporting Information

ABSTRACT: This novel, multi small-analyte sensing strategy is the result of combining the target-induced aptamer enzymatic protection approach with the CGE-LIF (capillary gel electrophoresis with laser-induced fluorescence) technique. The implemented assay principle is based on an analysis of the phosphodiesterase I (PDE I)-mediated size variation of a fluorescein-labeled aptamer (FApt), the enzyme catalyzing the removal of nucleotides from DNA in the 3′ to 5′ direction. In the absence of the target, the unfolded aptamer was enzymatically cleaved into short DNA fragments. Upon target binding, the DNA substrate was partially protected against enzymatic hydrolysis. The amount of bound aptamer remaining after the exonuclease reaction was proportional to the concentration of the target. The CGE technique, which was used to determine the separation of FApt species from DNA digested products, permitted the quantification of adenosine (A), ochratoxin A (O), and tyrosinamide (T) under the same optimized enzymatic conditions. This assay strategy was subsequently applied to the simultaneous detection of A, O, and T in a single capillary under buffered conditions using corresponding FApt probes of different lengths (23, 36, and 49 nucleotides, respectively). Additionally, the detection of these three small molecules was successfully achieved in a complex medium (diluted, heat-treated human serum) showing a good recovery. It is worth noting that the multiplexed analysis was accomplished for targets with different charge states by using aptamers possessing various structural features. This sensing platform constitutes a rationalized and reliable approach with an expanded potential for a high-throughput determination of small analytes in a single capillary.

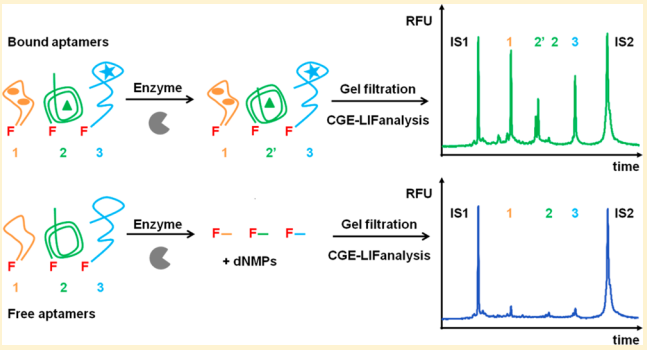

The capillary electrophoresis (CE) assay based on biological molecular recognition elements (MREs) known as an affinity probe capillary electrophoresis (APCE) assay provides a valuable analytical tool that combines the separation power of CE and the ligand specificity and affinity of biomolecules to detect analytes. Most previous papers on this approach, which has been under successful development for the past two decades, have used antibodies[1] or aptamers[2] as MREs. Compared with conventional analytical techniques, the CE method offers a number of advantages including automation, simplicity (by virtue of its homogeneous format), low sample consumption, and the flexibility to develop assays using various modes and formats. The following introduction focuses on existing APCE assays that are designed for simultaneous small-molecule determination.

CE-LIF-based affinity assays can be performed in either a competitive or a noncompetitive (direct) format. In direct affinity APCE-LIF assays, the labeled-MRE acts as a tracer, and an excess amount of this tracer is added to the sample to ensure the complete binding of analyte present in the reaction mixture. Analyte detection involves the efficient separation of both free and bound tracer based on their respective differences in size and charge. This separation is difficult to achieve because the binding of a small molecule generally does not significantly change the electrophoretic mobility of a labeled MRE. The use of labeled antibodies as tracers is limited because they are relatively heterogeneous[3,4] in comparison with nucleic acid aptamers, which can be easily modified and purified. However, constructing a simple direct assay format applicable to the simultaneous analysis of small molecules remains an unmet challenge. In competitive CE-based immunoassays, a labeled antigen competes with the antigen in the sample to bind to a limited amount of the corresponding antibody. Although, in principle, the direct format provides higher analytical performances, the competitive format is described more frequently because it offers (i) a significant change in the mobility of any small analyte upon binding to a large antibody and (ii) it

Received: November 30, 2013
Accepted: April 9, 2014
Published: April 9, 2014

   dx.doi.org/10.1021/ac5010234 | *Anal. Chem.* 2014, 86, 4233−4240

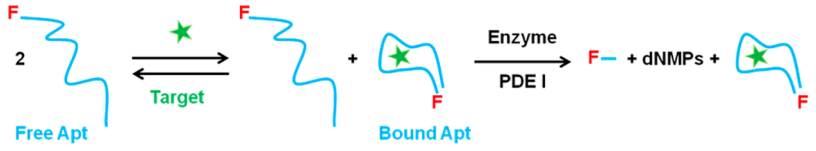

Figure 1. Target-induced aptamer enzymatic cleavage protection strategy. Although the unfold aptamer is enzymatically cleaved into very short DNA fragments by PDE I, the bound DNA substrate is protected against enzymatic hydrolysis by complexation with the target.

Table 1. List of Oligonucleotides Used[a]

names	sequences
FApt23-A	5′-CTGGGGGAGTATTGCGGAGGAAG-3′
F4-A	5′-CTGG
F3-A	5′-CTG
F2-A	5′-CT
F1-A	5′-C
FApt36-O	5′-GATCGGGTGTGGGTGGCGTAAAGGGAGCATCGGACA-3′
FApt31-O	5′-GATCGGGTGTGGGTGGCGTAAAGGGAGCATC-3′
FApt49-T	5′-AATTCGCTAGCTGGAGCTTGGATTGATGTGGTGTGTGAGTGCGGTGCCC-3′
12F IS[b]	5′-CCCAGGTTCTCT-3′
49F IS[b]	5′-AATTCGCTAGCTGGAGCTTGGATTGATGTGGTGTGTGAGTGCGGTGCCC-3′
65F IS[b]	5′-TGTGAGCCTCCTGTCGAAGGGGATGGACCCCTACTTCATTCGCCCGCCTTG AGCGTTTATTCTTG-3′

[a]Individual fluorescein labeling sites are underlined. [b]The 3′-end labeled DNA sequences, protected against enzymatic hydrolysis, were used as internal standards (IS).

facilitates the preparation of a uniform tracer. For practical reasons, because it is difficult to differentiate the various complexes, multianalyte immunoassays are based on monitoring the peak changes of free tracers. The multiple small-molecule approach has mainly been performed in capillary zone electrophoresis mode,[5−7] but effective electrophoretic separation sometimes makes it necessary (i) to work under micellar electrokinetic chromatography (MEKC) conditions[8] or (ii) to change the nature of the linked dye to modulate the tracer charge.[7] The competitive binding methodology described above is effectively applicable to CE-based aptamer assays, as previously demonstrated by our group.[9] In addition, studies have confirmed the simultaneous detection of multiple analytes using aptamers as MREs based on the complementary strand displacement approach,[10] which makes it possible to determine two small molecules in a single run by monitoring the target-induced duplex-to-complex change.[11] Nevertheless, all currently reported competitive multianalyte formats exhibit inherent drawbacks, including, for example, the difficulty to adequately design multiple probes[11−13] and the problem of tracers interfering with each other as the result of a potential complex dissociation that can occur during the course of electrophoresis. There exists thus a need to explore alternative strategies to these conventional APCE assays for the multiplexed determination of small analytes in a single capillary.

Earlier studies have reported that the binding of a target protein to its specific aptamer is able to protect, at least in part, the nucleic acid sequence from nuclease cleavage thanks to steric hindrance effects and conformational changes.[14−16] This feature has been successfully exploited for protein detection[14,16] and small molecule sensing;[17] it has also recently been extended to potassium ion sensing.[18] Early methods that used the target-induced aptamer enzymatic cleavage protection strategy were laborious, complicated, and time-consuming.[14,16] More recent assays using signal transduction strategies such as fluorescence anisotropy[17] and intensity[18] required dye molecules that possess distinct spectral features to implement a multianalyte assay. The novel approach we propose in this paper combines the simplicity and general applicability of the aptamer enzymatic cleavage protection concept (depicted in Figure 1) with the versatility and high-resolving power of CGE-LIF (capillary gel electrophoresis with laser-induced fluorescence). We used 5′-end fluorescein-labeled aptamers (FApt) as probes and phosphodiesterase I (PDE I) as the enzyme reagent to catalyze the removal of nucleotides from DNA in the 3′ to 5′ direction.[19] The assay was performed using three different systems corresponding to the small molecule targets adenosine (A), ochratoxin A (O), and tyrosinamide (T) and their respective DNA aptamers.[20−23] In essence, our method relies on a CE analysis of the PDE I-mediated size variation of the labeled aptamer probe using a poly(ethylene glycol) polymer matrix loaded into a coated capillary. We successfully separated FApt from the digested products generated by the enzymatic reaction. The amount of FApt protected against PDE I activity by target complexation was proportional to the target concentration, allowing us to independently determine A, O, and T under the same optimized enzymatic conditions. This assay strategy was subsequently applied to the simultaneous detection of the three small molecules in a single capillary under buffered and complex (diluted human serum) media conditions.

EXPERIMENTAL SECTION

Chemicals and Oligonucleotides. The following were obtained from Sigma-Aldrich (Saint-Quentin, France): β-D-adenosine (A), ochratoxin A (O), L-tyrosinamide (T), phosphodiesterase I type IV from *Crotalus atrox* (PDE I), tris(hydroxymethyl)aminomethane (Tris), poly(ethylene oxide) (PEO, MW = 1,000,000), poly(ethylene glycol) (PEG, MW = 35,000), urea, Sephadex G-25, and human serum (male, AB). NaCl and $MgCl_2 \cdot 6H_2O$ were purchased from Chimie-Plus laboratories (Bruyères de Pouilly, France) and Panreac Quimica

dx.doi.org/10.1021/ac5010234 | Anal. Chem. 2014, 86, 4233−4240

(Barcelona, Spain), respectively. HCl and NaOH were provided by Carlo Erba (Val de Reuil, France). Water was purified using a Purite Still Plus system (Thame, U.K.) fitted with a reverse osmosis cartridge.

The modified DNA was synthesized, HPLC-purified, and identified with MALDI-TOF mass spectrometry from Eurogentec (Angers, France). We labeled the oligonucleotides at one extremity with fluorescein (F) using a hexyl carbon linker and named them according to their length and the position of the dye. The aptamers were 5′-labeled and named according to their specific target. Sequences of all oligonucleotides used are listed in Table 1.

CE-LIF Equipment. An Agilent capillary electrophoresis system (Agilent Technologies, Waldbronn, Germany) equipped with a ZETALIF Discovery laser-induced fluorescence detector (Picometrics, Toulouse, France) adapted for a diode laser source (DPSS Laser Kyma 488 nm, Melles Griot, USA) was used throughout. We employed an uncoated fused-silica capillary with an inside diameter (i.d.) of 50 μm and an outside diameter (o.d.) of 362 μm (total length equals 59 cm; effective length equals 19 cm) equipped with a specific Discovery cell including an ellipsoid lens for the "on-capillary" collection of emitted light (Picometrics).

Capillary Coating and Electrophoresis Experiments. Before use, the fused-silica capillary was coated daily with PEO. This capillary wall treatment is adapted from previous studies.[24,25] First, the internal surface of the capillary was briefly pretreated at 1 bar with 1 M HCl solution for 10 min. The acidic solution was left in the capillary for 5 min before rinsing with pure water for 20 min. The capillary wall was then coated by flushing at 8 bar with 1% (w/v) PEO dissolved in a 1 M HCl solution for 50 min and with 1% (w/v) PEO dissolved in the running buffer for 10 min. The running buffer was composed of 20 mM Tris-HCl at pH 7.5 and 10 mM NaCl. Thereafter, the capillary was ready for an entire day. Prior to injection, for the A single-analyte and multiplexed sensing, the capillary was filled at 8 bar for 3 min with a linear polymer solution consisting of 10% (w/v) PEG and a running buffer containing 1 M urea, which allowed us to perform a size-dependent separation of the DNA strands. During the run, the capillary ends were kept in the latter separation solution. All experiments were carried out in anionic mode. Unless otherwise stated, samples were hydrodynamically injected into the capillary in duplicates at −50 mbar for 32 s. The CGE conditions were as follows: applied voltage of +15 kV and capillary cassette temperature of 35 °C. To ensure repeatability, the coated surface of the column was restored between runs by flushing at 8 bar with a running buffer containing 1% PEO for 5 min. Thereafter, the 10% PEG sieving medium was reloaded into the capillary. In this manner, we were able to conduct each run on a fresh separation solution. At the end of the day, the PEO coating was removed by consecutively flushing at 8 bar with the following: 1 M HCl solution for 10 min, water for 5 min, 1 M NaOH for 10 min, and water for 5 min. Stored at 4 °C, PEO solutions remained usable for at least 2 weeks. The PEG sieving matrix was prepared every day. Prior to use, all solutions were filtered through membranes with a pore size of 0.2 μm. We studied intraday (n = 10) and interday (4 days, 3 injections per day) migration time repeatability under the optimal CGE conditions described above. The migration time relative standard deviation (RSD) of less than 1% for FApt23-A and 49F IS allowed us to obtain good repeatability, demonstrating the stability of the nonbonded PEO coating. For O and T single-analyte sensing, the CGE conditions were slightly modified as described in the figure captions (see Supporting Information).

Single-Analyte Sample Preparation. The 1× incubation buffer consisted of 10 mM Tris-HCl at pH 8.5, 50 mM NaCl, and 10 mM $MgCl_2$. We dissolved the analytes (A, O, T), the DNA strands, and the PDE I (initial enzyme concentration C_0, 2 mU/μL) stock solutions in pure water and stored them at −20 °C. Prior to use, water and buffer were filtered through membranes with a pore size of 0.2 μm. We first prepared concentrated 4× aptamer solutions by diluting the stock solutions in a concentrated 4× incubation buffer and then heated the solutions at 80 °C for 5 min after which they were left standing at room temperature for 5 min in the dark. Thereafter, we prepared 41 μL of the sample solutions by mixing 12.5 μL of the concentrated 4× aptamer solution with different amounts of target. The resulting solutions were kept at 4 °C for at least 30 min to attain mixture equilibrium prior to the addition of 9 μL of PDE I C_0/1000. The enzymatic digestion was performed under the following optimized conditions: 25 °C in the 1× incubation buffer in the presence of an 18×10^{-6} U of PDE I in the solution. After 30 min of reaction, we added into the samples 30 μL of a 5.34 M urea solution dissolved in the 1× incubation buffer. The reaction was consequently stopped by concomitant dilution (1/1.6) of the samples in a denaturing solution. The IS strand, which we mixed to the urea solution, was used to monitor volume injection variability and coating stability. The samples were composed of fluorescein-labeled aptamers at a final concentration of 625 nM for A sensing and 312.5 nM for O and T sensing in a 1× incubation buffer containing 2 M urea (IS oligonucleotide concentration values are given in the figure captions). For the titration curves obtained from the single-analyte assay, the final analyte concentration varied from 0 to 3.5 mM for A and T and from 0 to 35 μM for O. The samples were kept at −20 °C until CE analysis.

Multiplex Sample Preparation. Samples were prepared as described above using a mixture of the three aptamers and of their respective targets to obtain the following final oligonucleotide concentrations: 500 nM for FApt23-A, 250 nM for FApt36-O and FApt49-T, 840 nM for 65F IS, and 300 nM for 12F IS. The enzymatic reaction was performed for 60 min in the presence of 36×10^{-6} U of PDE I to ensure the complete digestion of unbound oligonucleotides. We stopped the reaction by adding the urea solution containing the 65F IS strand to the samples. The working solutions were purified by gel filtration on Sephadex G-25 columns to remove the shortest digested fragments (2 mL of gel was used per sample). Thereafter, 50 μL of the resulting solutions was diluted (1/1.25) by adding 12.5 μL of a 12F IS solution dissolved in water. The 65F IS strand served to calculate the yield of the steric exclusion process. The 12F IS oligonucleotide was used to compensate for variations in the injection volume during the CGE analysis (see below). Both native and heat-treated (90 °C for 10 min, centrifugation and supernatant recovery) diluted human serum samples were used to test the performance of the multiplexed assay under biological conditions. Serum was diluted to a ratio of 1/25 during the enzymatic digestion (final dilution 1/50). We prepared the samples in duplicates to determine the recoveries obtained with native and heat-treated serum media.

dx.doi.org/10.1021/ac5010234 | Anal. Chem. 2014, 86, 4233−4240

RESULTS AND DISCUSSION

Optimization of the CGE Separation. CGE is principally used for the size-based separation of macromolecules such as proteins and nucleic acids.[26,27] The size separation is obtained by electrophoresis of the solutes, which uses a suitable polymer that acts as a "molecular sieve" thanks to its dynamic pore structure. Because charged solutes migrate through the polymer network, larger solutes are hindered to a greater extent than smaller solutes. Polyanionic oligonucleotides cannot be separated without a gel or without a drag-tag molecule in free solution[11] because they display similar charge-to-mass ratios. The separation mechanism of DNA by CGE requires the reduction of the electroosmotic flow (EOF), which can expel the sieving matrix from the bare fused-silica capillary. In addition, even when the EOF is slow, the flow's direction is opposite to the migration direction of DNA fragments, which leads to long separation times.

Capillaries coated by covalent wall passivation are commercially available, but (i) they are usually expensive and (ii) their bonded coating has a tendency to degrade over time. Fung and Yeung have reported that linear and neutral polymer PEO is "self-coating" by physically adsorbing on the internal capillary wall.[28] The adsorbed PEO coating, obtained through treatment with an acidic solution containing 0.2% of the high-molecular mass PEO (MW = 8 million), proved to reduce EOF velocity by more than 1 order of magnitude compared with the bare capillary, from pH 7.0 to 7.7. During electrophoresis, the coating exhibited high stability over time.[24] We were able to achieve an efficient EOF decrease from pH 7.0 to 7.5 by treating the internal capillary surface with a 1% PEO solution (MW = 1 million) and regenerating the coating between runs (see Experimental Section). Above pH 7.5, an immediately observable, gradual increase in oligonucleotide migration time over consecutive runs indicated that the coating degraded slowly.[24] Note that the low-molecular mass PEG (MW = 35,000), which is structurally almost identical to PEO, was unable to form a stable coating because of its shorter chain.[25]

Previous studies have shown that matrices prepared from PEO or PEG can serve as an effective sieving material for DNA sequencing and oligonucleotide analysis based on CGE, thereby providing single-base resolution and high reproducible separation performance for single-stranded DNA fragments.[28,29] In the present study, we examined the composition of the polymer solution (which determines the pore size of the polymeric entangled network), the capillary temperature, and the addition of a denaturant in order to increase the resolving power of the sieving matrix. We measured the separation performance by injecting a solution composed of three fluorescent aptamers possessing different lengths (23, 36, and 49 nucleotides). The FApt peaks were well resolved in matrices prepared from either an individual PEG or PEO polymer or from mixtures of both polymers dissolved in the running buffer. Similar to the results obtained for other polymers,[27] we observed that higher solution concentrations of a single polymer improved resolution. In contrast, mixed-polymer matrices possessing higher viscosity did not improve the separation performance due to a broadening of the peak shape. A 10% PEG solution provided adequate resolution values not only for the probes (17.7 and 11.2 for the FApt23-A/FApt36-O and FApt36-O/FApt49-T pairs, respectively) but also for all digested products resulting from enzymatic hydrolysis (see below). In the presence of urea, which was added to both the separating matrix and the samples, we were able to observe an improved efficiency by releasing the secondary structure of Apt. We further investigated the effects of the capillary temperature, which is known to strongly influence the performance of the separation, in a temperature range of 25 to 40 °C.[29] We found that the optimal separation temperature was dependent on PEG concentration, that is at 35 °C for a 10% PEG sieving matrix containing 1 M urea. The presence of urea in the running solution combined with a moderate temperature during the analysis ensured that oligonucleotides were separated by size as denatured single-stranded fragments, minimizing Apt secondary structure formation and preventing the hybridization of digestion products with complementary sequences.

Single-Analyte Sensing. Our group has previously demonstrated an assay principle based on the target-induced aptamer enzymatic cleavage protection strategy (Figure 1) for small molecule sensing using fluorescence polarization (FP) as a transduction technique.[17] In the present study, experimental parameters were initially optimized through FP for the three recognition systems studied (A/FApt23-A, O/FApt36-O, and T/FApt49-T). Details of the FP experiments (performed to determine the optimal incubation buffer composition, the pH and temperature of the enzymatic digestion, and the quantity of PDE I) are presented in the Supporting Information for the A/FApt23-A system[20,21] (Figure S1, Supporting Information). Optimized experimental conditions were similar for the three studied systems (i.e., 10 mM Tris-HCl pH 8.5, 50 mM NaCl, and 10 mM $MgCl_2$ at 25 °C).

We expect that this assay could be carried out using the CGE-LIF technique by monitoring the FApt signal change. CGE could make it possible to isolate the amount of bound aptamer that is left over from side-products following the exonuclease reaction, and the signal of FApt should be proportional to the target concentration. Our initial investigation of the feasibility of the single-analyte sensing approach was based on the antiadenosine DNA aptamer FApt23-A as a modeling system. We first monitored the PDE I-mediated FApt23-A digestion pattern for reaction times ranging from 2 min to 2 h with the optimized CGE-LIF method and in the absence of the target (Figure S2, Supporting Information). Electropherogram S2a was obtained by analyzing the FApt23-A and 49F IS mixture incubated with the denatured enzyme. In this case, digestion of the FApt23-A probe did not take place. Depending on their respective lengths and on the CGE mode used, the migration time of the aptamer (peak **2**) was lower than that of the 49F IS (peak **4**). For relatively short enzymatic reaction times (from 2 to 15 min), the FApt23-A band intensity decreased, and several peaks (**1**) appeared at lower migration times (Figure S2b–d, Supporting Information). This is in accordance with a typical partial digestion profile of oligonucleotides.[30−33] Initially, the PDE I enzyme successively hydrolyzed 5′-mononucleotides from the 3′-extremity in a nonprocessive manner; it then yielded a series of DNA fragments of lower length: *N*-1, *N*-2, *N*-3, ..., where *N* is the initial number of nucleotides.[30,31] As the reaction time increased (30 min), peaks of both the intact aptamer (**2**) and the digested products (**1**) almost disappeared (Figure S2e, Supporting Information). As previously reported,[30,31] such behavior is consistent with a complete digestion pattern, where the full-length oligonucleotide and the high molecular weight digestion intermediates are almost entirely hydrolyzed. Moreover, at the same time, two major peaks (**3** and **5**) appeared at

dx.doi.org/10.1021/ac5010234 | Anal. Chem. 2014, 86, 4233−4240

high migration times (Figure S2e, Supporting Information). We performed two separate experiments to fully elucidate the nature of these low velocity species. First, digests resulting from the enzymatic reaction were subjected to gel filtration on a Sephadex G25 column, and the resulting gel-filtered solutions were analyzed through CGE-LIF. In this case, peaks **3** and **5** disappeared from the electropherogram (data not shown), which is consistent with the removal of the corresponding fluorescein conjugates. This observation reveals that peaks **3** and **5** can be assigned to small fluorescent species containing only a few nucleotides. To gain further insight, we subsequently investigated the migration behavior of four 5′-end-fluorescein-DNA conjugates that consist of the four (F4-A), three (F3-A), two (F2-A), and one (F1-A) terminal bases from the 5′-extremity of the Apt-23 sequence, respectively (Table 1). The migration order of the four species was as follows: F4-A < F3-A < F2-A < F1-A. The migration time of the F4-A probe was identical to the migration time of the 12F IS strand, whereas F3-A showed a migration time close to that of FApt23-A (data not shown). More significantly, bands of the F2-A and F1-A species coincided with peaks **3** and **5**, respectively (Figure S2g, Supporting Information). This result confirms that the two major products of long digestion times correspond to very short fragments: di- and mononucleotides for peaks **3** and **5**, respectively. Moreover, for a very long reaction time (2 h), the F1-A mononucleotide (peak **5**) constituted the major fluorescent digestion product (Figure S2f, Supporting Information), consistent with a fully achieved oligonucleotide hydrolysis in the 3′ → 5′ direction.[30,31] The F1-A, F2-A, and F3-A conjugates showed a rather surprising migration behavior considering that very short fragments should migrate with high mobility under the present CGE mode. It is, however, well-known that oligonucleotide labeling can significantly affect the frictional forces of the entire species (and then shift the DNA mobility)[34,35] as the result of (i) the dye's intrinsic physicochemical features and (ii) the presence of the linker.[34] This effect seemed especially significant for species of very short length (≤3 nucleotides) for which the label contribution to the overall conjugate mobility became preponderant. The same migration behavior has previously been reported in gel electrophoresis-based dye-terminator sequencing for unreacted fluorescent dye-labeled dideoxynucleoside-triphosphates, which comigrated with sequencing products of longer length.[36]

We subsequently studied the effects of target (A) addition on the FApt23-A digestion pattern (Figure 2). A reaction time of 30 min was selected to obtain a minimal background signal of FApt23-A (Figure S2e, Supporting Information) without compromising the ability of the bound aptamer to resist digestion (Figure S1, Supporting Information). As the concentration of A increased in the reaction mixture, the aptamer peak (**2**) grew in both height and area, consistent with the target-induced aptamer cleavage protection mechanism (Figure 2c,d). Predictably, the magnitude of the short di- and mononucleotidic digestion products (peaks **3** and **5**) decreased at the same time. We also observed a small peak (**1**) appearing before the FApt23-A peak (Figure 2c,d). As PDE I degraded the unbound probe (Figure 1), the free form of FApt23-A progressively disappeared from the mixture during the course of the enzymatic reaction. This led to a displacement of the equilibrium between bound and free aptamers toward the unbound aptamer. This additional amount of free aptamer was then subjected to a nonprocessive enzymatic attack but only during a reduced reaction time, so that the weakly digested

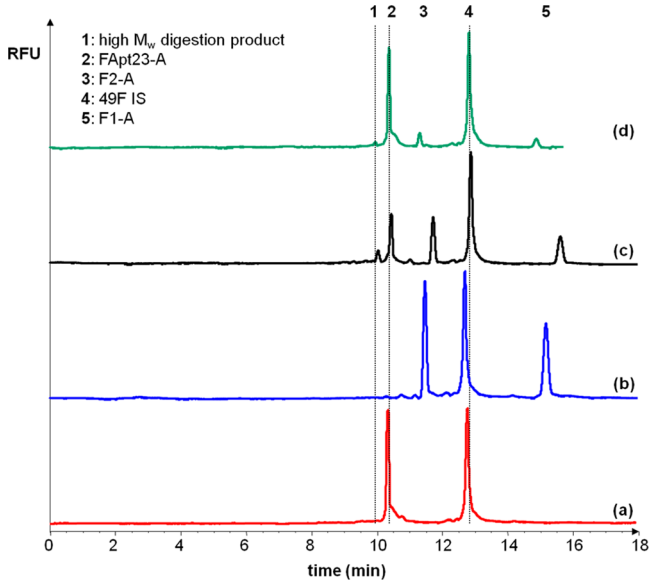

Figure 2. Representative electropherograms for adenosine (A) sensing obtained with the target-induced aptamer enzymatic cleavage protection strategy and for different concentrations of analyte: (a) 0 (+ denatured PDE I), (b) 0, (c) 60, and (d) 610 μM of A. Enzymatic reaction: 30 min at 25 °C. Sample composition: 625 nM FApt23-A for (a), 600 nM 49F IS, 18 × 10^{-6} U of PDE I in 10 mM Tris-HCl pH 8.5, 50 mM NaCl, 10 mM $MgCl_2$, and 2 M urea. Separation matrix: 10% PEG in 20 mM Tris-HCl pH 7.5, 10 mM NaCl, and 1 M urea. Injection conditions: 32 s, −50 mbar. Separation conditions: 15 kV, 35 °C, PEO coating.

product (of high molecular weight) was formed. Moreover, peak **1** intensity decreased significantly with A concentration increasing (Figure 2c vs Figure 2d) due to the limited target-aptamer complex dissociation that occurred at high target concentration. We calculated the FApt23-A to 49F IS peak area ratios (RSD values ≤5%). The FApt23-A peak area of the sample containing denatured PDE I corresponded to the highest oligonucleotide concentration (Figure 2a). Thus, the FApt to 49F IS peak area ratio was considered equal to 100%. We then established the titration curves by plotting the percentage of undigested FApt vs the target concentration (Figure 3). Assay response increased linearly as the A concentration increased from 0 to 70 μM. The detection limit (LOD) was estimated using the calculation method based on the slope of calibration curve and the SD (×3) of blank response (n = 6, intraday and interday experiments). We obtained a LOD of 8 μM, which is in the same range as those typically reported with fluorescent aptasensing methods (excluding amplification-based biosensors).[17,21,37−40]

We then evaluated the generalizability of our approach under the exact same reaction conditions for the two other recognition systems, O/FApt36-O and T/FApt49-T (Figures S3−S6, Supporting Information). As for the A system, digestion of the O aptamer probe and intermediates was mostly completed in the absence of the target (Figure S3b, Supporting Information). For the T system, both FApt49-T and high molecular weight digestion products were still observed because of the longer DNA sequence to cleave (Figure S4b, Supporting Information). Nevertheless, upon target addition, the labeled aptamer peak grew in area for the two systems, which is consistent with the enzymatic cleavage protection mechanism (Figures S3c,d and S4c,d, Supporting

dx.doi.org/10.1021/ac5010234 | Anal. Chem. 2014, 86, 4233−4240

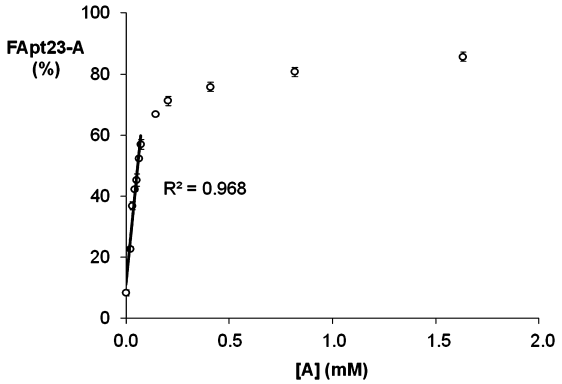

Figure 3. Titration curve obtained for the aptamer probe FApt23-A with increasing adenosine (A) concentrations. Sample composition and CGE conditions are given in Figure 2 (legend). Error bars represent standard deviations (n = 2). Curves are constructed by plotting the percentage of undigested aptamer corresponding to the FApt23-A to 49F IS peak area ratio with respect to the FApt23-A/49F peak area ratio of initial oligonucleotide concentrations vs the analyte concentration.

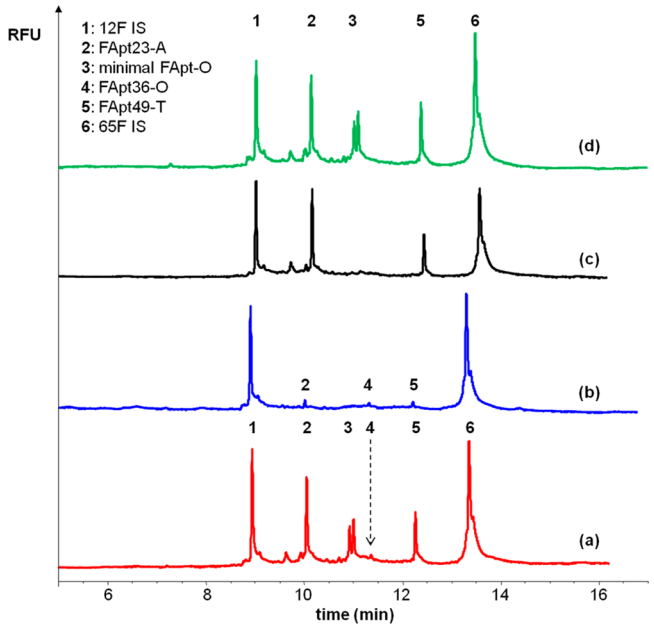

Figure 4. Representative electropherograms of the target-induced aptamer enzymatic cleavage protection assay for multianalyte sensing: adenosine (A), ochratoxin A (O), and tyrosinamide (T). Sample target compositions: (a), (c), (d) 160 μM of A, 2 μM of O, and 650 μM T; (b) no analytes. Samples under either buffered solution conditions (a, b), 50-fold diluted native human serum conditions (c), or heat-treated diluted human serum (1/50) conditions (d). Enzymatic reaction conditions and sample preparations are given in the Experimental Section. Separation matrix: 10% PEG in 20 mM Tris-HCl pH 7.5, 10 mM NaCl, and 1 M urea. Injection conditions: 16 s, −50 mbar. Separation conditions: 15 kV, 35 °C, PEO coating.

Information). Note that we specifically used the peak of the minimal protected aptamer sequence instead of the sequence of the whole FApt36-O probe to construct the O target titration curve (see Supporting Information for details). We established the titration curves for the two systems possessing increasing O and T concentrations (Figures S5 and S6, Supporting Information). Our subsequent analysis of the assay performance provided an LOD of 26 μM and 140 nM and a linearity range of up to 300 μM (R^2 = 0.972) and 700 nM (R^2 = 0.995) for T and O, respectively. These detection limits are satisfactory compared with those observed with most fluorescence-based aptasensors for these two analytes.[17,41−44]

We presume that the difference in analytical performance that we obtained for the three single-analyte assays mainly originated from (i) the difference in dissociation constant for the three complexes (ranging from ∼100 nM for O to ∼6 μM for A)[20,22,41] and from (ii) the distinct structural features of aptamers (hairpin-like, G-quadruplex, and undetermined motifs for FApt23-A, FApt36-O, and FApt49-T, respectively),[45−47] which could influence the DNA's susceptibility to enzymatic attack.

Multiplexed Analyte Sensing. As a preliminary step, we performed FP-based experiments to establish that the assay response for one analyte was unaffected by the presence of the other analytes (Figure S1e, Supporting Information), highlighting the lack of cross-reactivity between the three present sensing systems. In the following step, we therefore used the CGE mode for the simultaneous detection of the three small analytes in a single run (Figure 4). To ensure complete digestion of the larger amount of DNA under target-free conditions, the operating conditions were adapted by increasing both the reaction time and the amount of PDE I (see Experimental Section). Additionally, the working solutions resulting from the enzymatic reaction had been previously purified by gel filtration on Sephadex G25 columns to remove the short digested products. This gel filtration process also allowed us to decrease the ionic strength of the injected samples, resulting in a field-amplified sample stacking effect, which in turn improved separation efficiency. Whether or not the 65F IS-containing samples had been subjected to the gel filtration step, we compared the analytical results for both samples to evaluate the yield of this purification procedure. We determined a steric exclusion yield of greater than 95% by calculating the 65F IS/12F IS peak area ratios we obtained from these two experiments (data not shown). In the absence of targets (Figure 4b), the FApt probes were almost completely hydrolyzed, giving rise to very small peaks. As for the A single-analyte experiments (see above), no other significant peaks appeared in the electropherogram, confirming that the potentially interfering short digestion products were essentially eliminated during the gel filtration process. As shown in Figure 4a, high-intensity peaks corresponding to the full FApt23-A, FApt49-T, and minimal FApt-O sequence probes were observed in the presence of their respective targets, that is for a concentration of 160 μM, 2 μM, and 650 μM for A, O, and T, respectively. Note that the relatively enhanced separation efficiency with respect to the single-analyte format made it possible to differentiate the FApt-O tracers, leading to two separate bands (Figure 4a vs Figure S3d, Supporting Information).

Once the proof-of-principle of the multiplexed assay was established, we evaluated the suitability of the multisensing approach for a biological environment using 25-fold diluted human serum samples during enzymatic digestion (Figure 4c). Because of its known ability to reduce the adsorption of interfering proteins on the capillary wall during electrophoresis, a PEO coating is particularly adapted to obtaining reproducible separations with reliable and sharp signals.[25] In the presence of targets, we observed an increase in the FApt23-A (or FApt49-T) to 65F IS peak area ratio in the realistic medium compared with the buffered solution (Figure 4c vs Figure 4a), resulting in

dx.doi.org/10.1021/ac5010234 | Anal. Chem. 2014, 86, 4233−4240

slightly overestimated recoveries for the two species (121% and 111% for A and T, respectively, with RSD < 10%). We presume that the data originated from the differential, nonspecific interaction of the 65F IS oligonucleotide with the serum proteins.[48] The long 65F IS strand likely bound to proteins with greater affinity than the shorter FApt23-A and FApt49-T sequences, leading to distinct serum matrix interferences. Surprisingly, the FApt-O tracers were not visualized in the electropherogram (Figure 4c). Their absence may be attributed to the high-affinity binding of O to blood proteins, especially serum albumin.[49] In order to overcome these difficulties, the serum proteins were then heat-denatured prior to the enzymatic reaction (Figure 4d). After this treatment, the 65F IS signal was restored and the FApt-O probes were efficiently protected from enzymatic digestion, leading to an electrophoretic profile similar to that retrieved with the buffered solution (Figure 4d vs Figure 4a). Under these heat-denaturation conditions, we further observed recoveries in the 98−104% range (RSD typically ≤6%) for the three A/FApt23-A, O/FApt-O, and T/FApt49-T systems, indicating the practical applicability of this procedure.

CONCLUSION

In summary, we present a description of a novel, multi small-analyte sensing strategy that combines the target-induced aptamer enzymatic protection approach with the CGE-LIF technique, offering a promising alternative to conventional competitive APCE assays. This study represents the first example of multiplexed determination in a single solution based on the aptamer enzymatic protection concept. The present assay makes it possible to detect small molecules with three different charge states (cationic, neutral, and anionic) by using aptamers possessing distinct structural motifs,[45−47] which suggests a broad applicability of the approach. We expect that this sensing platform could be extended to other species classes from proteins to ions on the condition that a target-induced aptamer enzymatic protection occurs.[14,16,18] The high resolving ability of CGE combined with gel filtration-mediated sample stacking effects produce the significant peak capacity of this system, on the basis of which we envision a further potential to high-throughput analysis in a single capillary. It is conceivably possible to separate a greater number of specific aptameric probes by rationally manipulating their length. Unlike the typical multiplexed APCE methods, the current approach precludes interferences originating from the dissociation of each labeled tracer-MRE complex during the run, leading to more reliable results. Finally, as previously reported,[14,16] the analytical performance of the assay could potentially be improved by introducing an additional step for the PCR amplification of the protected strands following their sequential collection at the capillary outlet.[50,51]

ASSOCIATED CONTENT

Supporting Information

Figures S1−S6 and additional data as noted in the text. This material is available free of charge via the Internet at http://pubs.acs.org.

AUTHOR INFORMATION

Corresponding Author

*E-mail: Eric.Peyrin@ujf-grenoble.fr.

Notes

The authors declare no competing financial interest.

ACKNOWLEDGMENTS

This study received financial support from the ANR program "Labex Arcane" (ANR-11-LABX-0003-01). Z. Zhu was supported by the China Scholarship Council fund affiliated with the Ministry of Education of the P. R. China. We would like to thank A. Peronnon and J. R. Sevilla for their technical assistance.

REFERENCES

(1) Guzman, N. A.; Philipps, T. M. *Electrophoresis* **2011**, *32*, 1565−1578.
(2) Smuc, T.; Ahn, I. Y.; Ulrich, H. *J. Pharm. Biomed. Anal.* **2013**, *81*−*82*, 210−217.
(3) Schmalzing, D.; Nashabeh, W.; Fuchs, M. *Clin. Chem.* **1995**, *41*, 1403−1406.
(4) Chiem, N.; Harrison, D. J. *Anal. Chem.* **1997**, *69*, 373−378.
(5) Caslavska, J.; Allemann, D.; Thormann, W. *J. Chromatogr., A* **1999**, *838*, 197−211.
(6) Suzuki, Y.; Arakawa, H.; Maeda, M. *Anal. Sci.* **2003**, *19*, 111−115.
(7) Chen, F. T. A.; Evangelista, R. A. *Clin. Chem.* **1994**, *40*, 1819−1822.
(8) Steinmann, L.; Thormann, W. *Electrophoresis* **1996**, *17*, 1348−1356.
(9) Ruta, J.; Ravelet, C.; Baussanne, I.; Décout, J.-L.; Peyrin, E. *Anal. Chem.* **2007**, *79*, 4716−4719.
(10) Nutiu, R.; Li, Y. *J. Am. Chem. Soc.* **2003**, *125*, 4771−4778.
(11) Zhu, Z.; Ravelet, C.; Perrier, S.; Guieu, V.; Roy, B.; Périgaud, C.; Peyrin, E. *Anal. Chem.* **2010**, *82*, 4613−4620.
(12) Dunkle, M. N.; Herrmann, J. K.; Colón, H.; Pennington, C.; Colón, L. A. *Microchem. J.* **2006**, *82*, 100−107.
(13) Bromberg, A.; Mathies, R. A. *Anal. Chem.* **2003**, *75*, 1188−1195.
(14) Wang, X. L.; Li, F.; Su, Y. H.; Sun, X.; Li, X. B.; Schluesener, H. J.; Tang, F.; Xu, S. Q. *Anal. Chem.* **2004**, *76*, 5605−5610.
(15) Haes, A. J.; Giordano, B. C.; Collins, G. E. *Anal. Chem.* **2006**, *78*, 3758−3764.
(16) Lin, J. S.; McNatty, K. P. *Clin. Chem.* **2009**, *55*, 1686−1693.
(17) Kidd, A.; Guieu, V.; Perrier, S.; Ravelet, C.; Peyrin, E. *Anal. Bioanal. Chem.* **2011**, *401*, 3229−3234.
(18) Zheng, D.; Zou, R.; Lou, X. *Anal. Chem.* **2012**, *84*, 3554−3560.
(19) Razzell, W. E.; Khorana, H. G. *J. Biol. Chem.* **1959**, *234*, 2114−2117.
(20) Huizenga, D. E.; Szostak, J. W. *Biochemistry* **1995**, *34*, 656−665.
(21) Perrier, S.; Ravelet, C.; Guieu, V.; Fize, J.; Roy, B.; Périgaud, C.; Peyrin, E. *Biosens. Bioelectron.* **2010**, *25*, 1652−1657.
(22) Cruz-Aguado, J. A.; Penner, G. *J. Agric. Food Chem.* **2008**, *56*, 10456−10461.
(23) Vianini, E.; Palumbo, M.; Gatto, B. *Bioorg. Med. Chem.* **2001**, *9*, 2543−2548.
(24) Preisler, J.; Yeung, E. S. *Anal. Chem.* **1996**, *68*, 2885−2889.
(25) Iki, N.; Yeung, E. S. *J. Chromatogr., A* **1996**, *731*, 273−282.
(26) Heller, C. *J. Chromatogr., A* **1995**, *698*, 19−31.
(27) Albarghouthi, M. N.; Barron, A. E. *Electrophoresis* **2000**, *21*, 4096−4111.
(28) Fung, E. N.; Yeung, E. S. *Anal. Chem.* **1995**, *67*, 1913−1919.
(29) https://www.chem.agilent.com/Library/applications/on-analysis.pdf.
(30) Mao, B.; Li, B.; Amin, S.; Cosman, M.; Geacintov, N. E. *Biochemistry* **1993**, *32*, 11785−11793.
(31) Park, S.; Seetharaman, M.; Ogdie, A.; Ferguson, D.; Tretyakova, N. *Nucleic Acids Res.* **2003**, *31*, 1984−1994.
(32) Kasahara, Y.; Kitadume, S.; Morihiro, K.; Kuwahara, M.; Ozaki, H.; Sawai, H.; Imanishi, T.; Obika, S. *Bioorg. Med. Chem. Lett.* **2010**, *20*, 1626−1629.
(33) Kasahara, Y.; Irisawa, Y.; Fujita, H.; Yahara, A.; Ozaki, H.; Obika, S.; Kuwahara, M. *Anal. Chem.* **2013**, *85*, 4961−4967.

(34) Meagher, R. J.; McCormick, L. C.; Haynes, R. D.; Won, J. I.; Lin, J. S.; Slater, G. W.; Barron, A. E. *Electrophoresis* **2006**, *27*, 1702−1712.
(35) Hahn, M.; Wilhelm, J.; Pingoud, A. *Electrophoresis* **2001**, *22*, 2691−2700.
(36) Finn, P. J.; Sun, L.; Nampalli, S.; Xiao, H.; Nelson, J. R.; Mamone, J. A.; Grossmann, G.; Flick, P. K.; Fuller, C. W.; Kumar, S. *Nucleic Acids Res.* **2002**, *30*, 2877−2885.
(37) Xu, W.; Lu, Y. *Anal. Chem.* **2010**, *82*, 574−578.
(38) Xiang, Y.; Tong, A.; Lu, Y. *J. Am. Chem. Soc.* **2009**, *131*, 15352−15357.
(39) Liao, D.; Jiao, H.; Wang, B.; Lin, Q.; Yu, C. *Analyst* **2012**, *137*, 978−982.
(40) Zhu, Z.; Ravelet, C.; Perrier, S.; Guieu, V.; Fiore, E.; Peyrin, E. *Anal. Chem.* **2012**, *84*, 7203−7211.
(41) Cruz-Aguado, J. A.; Penner, G. *Anal. Chem.* **2008**, *80*, 8853−8855.
(42) Ruta, J.; Perrier, S.; Ravelet, C.; Fize, J.; Peyrin, E. *Anal. Chem.* **2009**, *81*, 7468−7473.
(43) Zhao, Q.; Lv, Q.; Wang, H. *Anal. Chem.* **2014**, *86*, 1238−1245.
(44) Sheng, L.; Ren, J.; Miao, Y.; Wang, J.; Wang, E. *Biosens. Bioelectron.* **2011**, *26*, 3494−3499.
(45) Lin, C. H.; Patel, D. J. *Chem. Biol.* **1997**, *4*, 817−832.
(46) Yang, C.; Wang, Y.; Marty, J. L.; Yang, X. *Biosens. Bioelectron.* **2011**, *26*, 2724−2727.
(47) Lin, P. H.; Yen, S. L.; Lin, M. S.; Chang, Y.; Louis, S. R.; Higuchi, A.; Chen, W. Y. *J. Phys. Chem. B* **2008**, *112*, 6665−6673.
(48) Zhang, D.; Zhao, Q.; Zhao, B.; Wang, H. *Anal. Chem.* **2012**, *84*, 3070−3074.
(49) O'Brien, E.; Dietrich, D. R. *Crit. Rev. Toxicol.* **2005**, *35*, 33−60.
(50) Yang, J.; Bowser, M. T. *Anal. Chem.* **2013**, *85*, 1525−1530.
(51) Zhang, H.; Wang, Z.; Li, X. F.; Le, X. C. *Angew. Chem., Int. Ed.* **2006**, *45*, 1576−1580.